

POTENTIAL MODEL FOR Σ_u^- HYBRID MESON STATE*

NOSHEEN AKBAR

Department of Physics, COMSATS University Islamabad
Lahore Campus, Lahore 54000, Pakistan
nosheenakbar@cuilahore.edu.pk, noshinakbar@yahoo.com

SABA NOOR

Centre For High Energy Physics, University of the Punjab
Lahore 54590, Pakistan
sabanoor87@gmail.com

(Received May 11, 2020; accepted July 6, 2021)

In this paper, lattice simulations are used to propose a potential model for gluonic excited Σ_u^- states of bottomonium meson. This proposed model is used to calculate radial wave functions, masses and radii of Σ_u^- bottomonium hybrid mesons. Here, the gluonic field between a quark and an antiquark is treated as in the Born–Oppenheimer approximation, and the Schrödinger equation is numerically solved employing the shooting method.

DOI:10.5506/APhysPolB.52.1105

1. Introduction

Static quark potential models play an important role in understanding of Quantum Chromodynamics. A hybrid static potential is defined as a potential of a static quark–antiquark pair with the gluonic field in the excited state. Hybrid static potentials for different states of mesons are computed in Refs. [1–5]. These hybrid static potentials are characterised by quantum numbers, Λ , η , and ϵ , where Λ is the projection of the total angular momentum of gluons and for $\Lambda = 0, \pm 1, \pm 2, \pm 3, \dots$, meson states are represented as Σ, Π, Δ , and so on respectively [1]. η is a combination of parity and charge, and for $\eta = P \circ C = +, -$, states are labelled by subscripts g, u [1]. ϵ is the eigenvalue corresponding to the operator P and is equal to $+, -$. Parity and charge for hybrid static potentials are defined as [1]

$$P = \epsilon(-1)^{L+\Lambda+1}, \quad C = \epsilon\eta(-1)^{L+\Lambda+S}. \quad (1)$$

* Funded by SCOAP³ under Creative Commons License, CC-BY 4.0.

The low-lying static potential states are labelled $\Sigma_g^+, \Sigma_g^-, \Sigma_u^+, \Sigma_u^-, \Pi_g, \Pi_u, \Delta_g, \Delta_u$ and so on [1]. Σ_g^+ is the low-lying potential state with ground state gluonic field and is approximated by a Coulomb plus linear potential. The Π_u and Σ_u^- are the $Q\bar{Q}$ potential states with low-lying gluonic excitations. Linear plus Coulomb potential model is extended for Π_u states in [6] by fitting the suggested ansatz with the difference of Π_u and Σ_g^+ states lattice data [5], and this extended model is tested by finding properties of mesons for a variety of J^{PC} states in Refs. [6–9]. In the present paper, the linear plus Coulomb potential model is extended for the lowest excited hybrid state, Σ_u^- , by fitting the difference of Σ_u^- and Σ_g^+ states lattice data [5] with a newly suggested analytical expression (ansatz). The validity of suggested ansatz is tested by calculating the spectrum of Σ_u^- states hybrid bottomonium and comparing it with lattice results. For this purpose, the Born–Oppenheimer formalism and adiabatic approximation are used. Relativistic corrections in the masses are incorporated through the perturbation theory.

Heavy hybrid mesons have been studied using theoretical approaches such as the lattice QCD [1–3, 5, 10], constituent gluon model [11–13], effective field theory [14], QCD sum rule [15–22] and Bethe–Salpeter equation [23].

The paper is organised as follows: In Section 2, the potential model for Σ_g^+ state is discussed, while the proposed potential model for Σ_u^- state is defined in Section 3. The methodology of finding radial wave functions, spectrum and radii is explained in Section 4, while the discussion on the results and concluding remarks are written in Section 5.

2. Potential model for Σ_g^+ states

Σ_g^+ is the quarkonium state with ground state gluonic field and the potential model for this state is defined as [24]

$$V(r) = \frac{-4\alpha_s}{3r} + br + \frac{32\pi\alpha_s}{9m_b m_{\bar{b}}} \left(\frac{\sigma}{\sqrt{\pi}} \right)^3 e^{-\sigma^2 r^2} \mathbf{S}_b \cdot \mathbf{S}_{\bar{b}} + \frac{4\alpha_s}{m_b^2 r^3} S_T + \frac{1}{m_b^2} \left(\frac{2\alpha_s}{r^3} - \frac{b}{2r} \right) \mathbf{L} \cdot \mathbf{S}. \quad (2)$$

Here $\frac{-4\alpha_s}{3r}$ describes coulomb like interaction while linear term br is due to linear confinement. The term with $\mathbf{S}_b \cdot \mathbf{S}_{\bar{b}}$ is equal to

$$\mathbf{S}_b \cdot \mathbf{S}_{\bar{b}} = \frac{S(S+1)}{2} - \frac{3}{4} \quad (3)$$

$\mathbf{L} \cdot \mathbf{S}$ describes the spin orbit interactions defined as

$$\mathbf{L} \cdot \mathbf{S} = [J(J+1) - L(L+1) - S(S+1)]/2. \quad (4)$$

S_T is the tensor operator defined in [24] as

$$\langle {}^3L_J | S_T | {}^3L_J \rangle = \begin{cases} -\frac{L}{6(2L+3)}, & J = L+1, \\ +\frac{1}{6}, & J = L, \\ -\frac{L+1}{6(2L-1)}, & J = L-1. \end{cases} \quad (5)$$

Here, L is the relative orbital angular momentum of the quark–antiquark and S is the total spin angular momentum. Spin-orbit and colour tensor terms are equal to zero [24] for $L = 0$. m_b is the constituent mass of bottom quark. To calculate the radial wave functions, parameters $\alpha_s = 0.36$, $b = 0.1340 \text{ GeV}^2$, $\sigma = 1.34 \text{ GeV}$, $m_b = 4.825 \text{ GeV}$ are taken from Ref. [8].

3. Potential model for Σ_u^- states

Static potentials computed by lattice simulations are plotted in Fig. 3 of Ref. [5] for Σ_g^+ , Π_u , and Σ_u^- states with respect to quark–antiquark separation (r). From this lattice data [5], the difference between Σ_g^+ and Σ_u^- potentials within a given range of r is calculated and fitted with the following ansatz:

$$V_\Sigma(r) = A' \exp(-B' r^{P'}) + C'. \quad (6)$$

The best fit values of the parameters A' , B' , P' and C' are obtained. The values of these four parameters with standard error are equal to

$$\begin{aligned} A' &= 11.5917 \pm 1.1514 \text{ GeV}, & B' &= 2.9224 \pm 0.0913, \\ P' &= 0.2810 \pm 0.0120, & C' &= 0.9589 \pm 0.0060 \text{ GeV}. \end{aligned} \quad (7)$$

Here, $V_\Sigma(r)$ represents the potential difference between the ground state and the hybrid Σ_u^- state. Hence, the potential for Σ_u^- state can be modelled as

$$V(r) + V_\Sigma(r). \quad (8)$$

$V(r)$ and $V_\Sigma(r)$ are defined in Eq. (2) and Eq. (6). χ^2 can be defined as

$$\chi^2 = \sum_{i=1}^n \left(\frac{\varepsilon_i - (A' \exp(-B' r_i^{P'}) + C')}{\delta \varepsilon_i} \right)^2. \quad (9)$$

Here, ε_i are the data points taken from Fig. 3 of lattice data [5] and $n = 42$ is the number of data points used in the fitting. These data points are shown in Fig. 1 (a). $\delta \varepsilon_i$ is the error/uncertainty in ε_i . In the present work, data points ($\delta \varepsilon_i$) are taken with large accuracy, so the error in their values is very small. Therefore, one may consider $\delta \varepsilon_i = \Lambda \varepsilon_i$ and the appropriate value of

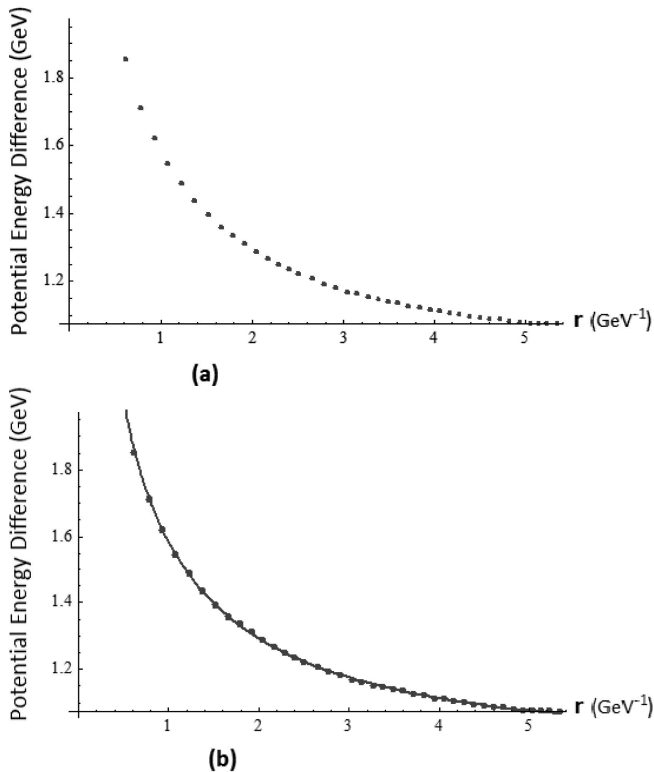


Fig. 1. (a) Data points for the potential difference between Σ_u^- and ground states. (b) Points represent the data points for the potential energy difference taken from Ref. [5] and the solid line represents our proposed model.

the factor Λ is calculated by using the following condition of the goodness of fit:

$$\frac{\chi^2}{n - a} = 1. \quad (10)$$

a represents the number of parameters used in the model. For the model defined in Eq. (6), Λ is calculated to be 0.0023664. If the number of parameters is reduced, the value of Λ increases as shown in Table I. This shows that the error/uncertainty in the ε_i increases with reduction of the number of parameters.

The fit of the proposed model ($V_\Sigma(r)$) with the difference of Σ_g^+ and Σ_u^- potential states lattice data is shown in Fig. 1 (b).

TABLE I

 Λ for different ansätze.

Ansatz	Λ	A'	B'	P'	C'
$A' \exp(-B' r_i^{P'}) + C'$	0.0023664	11.5917	2.9224	0.2810	0.9589
$A' \exp(-B' r_i^{P'})$	0.0350816	962.793	6.3795	0.044	—
$A' \exp(-B' r_i) + C'$	0.0241949	1.7609	1.2192	—	1.1042
$\exp(-B' r_i^{P'}) + C'$	0.042738	—	0.6379	1.6690	1.1302
$A' \exp(-r_i) + C'$	0.0236432	1.5694	—	1.0264	1.0798

4. Characteristics of Σ_u^- hybrid bottomonium states

4.1. Radial wave function of Σ_g^+ and Σ_u^- states

For Σ_g^+ state, the radial Schrödinger equation is written as

$$U''(r) + 2\mu \left(E - V(r) - \frac{L(L+1)}{2\mu r^2} \right) U(r) = 0, \quad (11)$$

where $V(r)$ is defined above in Eq. (2). Here, $U(r) = rR(r)$, where $R(r)$ is the radial wave function. To find numerical solutions of the Schrödinger equation for Σ_g^+ states, the shooting method is used. At the small distance ($r \rightarrow 0$), the wave function becomes unstable due to a very strong attractive potential. This problem is solved by applying smearing of position coordinates by using the method discussed in Ref. [25].

For Σ_u^- bottomonium hybrid states, the radial Schrödinger equation can be modified as

$$\begin{aligned} & U''(r) + 2\mu \\ & \times \left(E - V(r) - A' \exp(-B' r^{P'}) - C' - \frac{L(L+1) - 2\Lambda^2 + \langle J_g^2 \rangle}{2\mu r^2} \right) \\ & \times U(r) = 0. \end{aligned} \quad (12)$$

Here, $\langle J_g^2 \rangle$ is the square of gluon angular momentum and $\langle J_g^2 \rangle = 2$ [1] for Σ_u^- state. Λ is the projection of gluon angular momentum and $\Lambda = 0$ [1] for Σ_u^- state. Numerical solutions of the Schrödinger equation for Σ_u^- states are found with the same method as discussed above and resultant radial wave functions with different J^{PC} are shown in Fig. 2 and Fig. 3. The quantum numbers (L and S) for these states are given below in Table II.

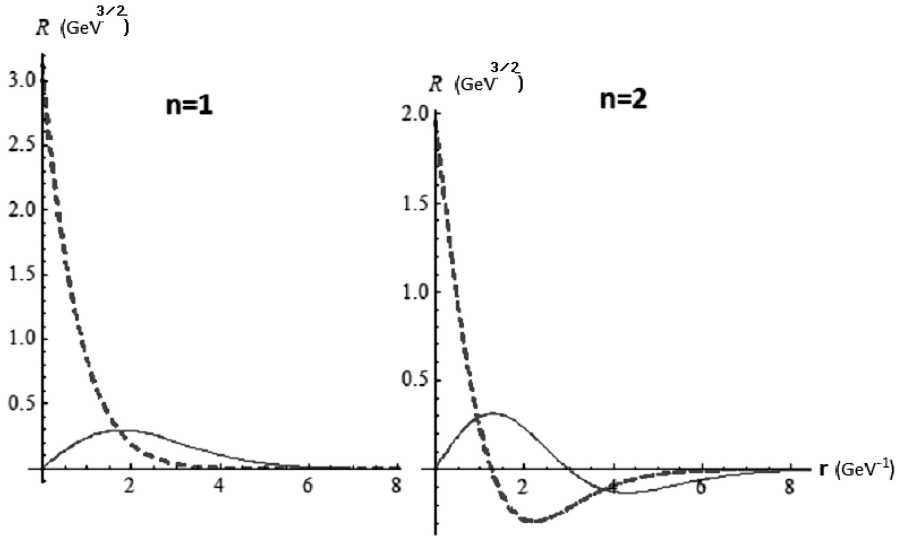


Fig. 2. The radial wave functions for Σ_g^+ and Σ_u^- states for $L = 0$. The solid lines indicate Σ_u^- states and the dashed curves are for Σ_g^+ states. Radial wave functions for $S = 0$ and $S = 1$ with $L = 0$ are almost the same in our numerical limits.

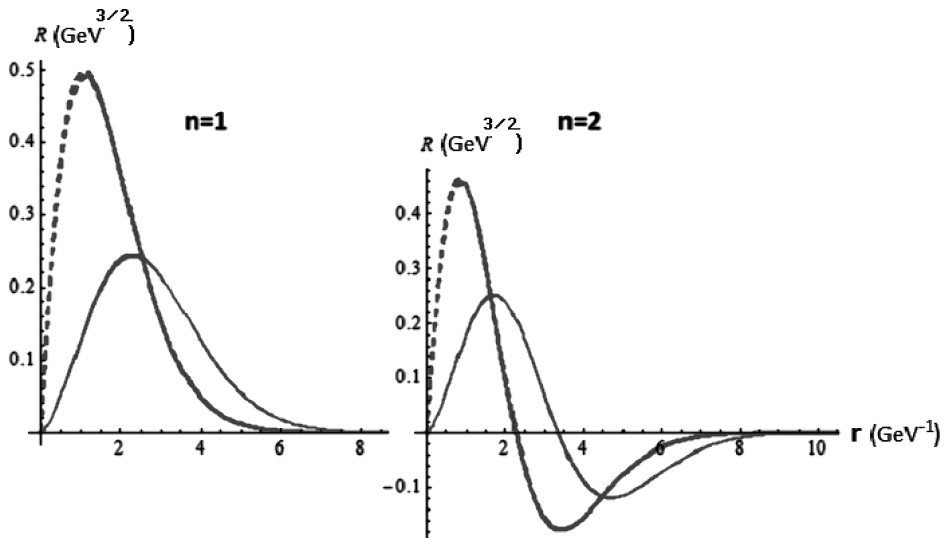


Fig. 3. The radial wave functions for Σ_g^+ and Σ_u^- states for $L = 1$. The solid lines indicate Σ_u^- states and the dashed curves are for Σ_g^+ states. Radial wave functions for $S = 0$ and $S = 1$ with $L = 1$ are almost the same in our numerical limits.

TABLE II

Our calculated masses of $b\bar{b}$ hybrid Σ_u^- bottomonium mesons.

Meson	J^{PC}	Calculated mass		Mass [3]	Calculated $\sqrt{\langle r^2 \rangle}$
		Relativistic	NR		
		GeV	GeV	GeV	fm
$\eta_b^h(1^1S_0)$	0^{++}	11.2378	11.2012	10.912(3)	0.5827
$\Upsilon^h(1^3S_1)$	1^{+-}	11.2385	11.2018		0.5841
$\eta_b^h(2^1S_0)$	0^{++}	11.4244	11.4154	11.192(5)	0.8375
$\Upsilon^h(2^3S_1)$	1^{+-}	11.4254	11.4163		0.8392
$\eta_b^h(3^1S_0)$	0^{++}	11.5911	11.6079		1.0562
$\Upsilon^h(3^3S_1)$	1^{+-}	11.5922	11.6089		1.0580
$\eta_b^h(4^1S_0)$	0^{++}	11.7440	11.7853		1.2539
$\Upsilon^h(4^3S_1)$	1^{+-}	11.7451	11.7864		1.2555
$\eta_b^h(5^1S_0)$	0^{++}	11.8866	11.9514		1.4369
$\Upsilon^h(5^3S_1)$	1^{+-}	11.8876	11.9526		1.4385
$\eta_b^h(6^1S_0)$	0^{++}	12.0210	12.1086		1.6090
$\Upsilon^h(6^3S_1)$	1^{+-}	12.0219	12.1098		1.6105
$h_b^h(1^1P_1)$	1^{--}	11.2983	11.2689	10.998(4)	0.6574
$\chi_0^h(1^3P_0)$	0^{-+}	11.2928	11.2645		0.6873
$\chi_1^h(1^3P_1)$	1^{-+}	11.2976	11.2684		0.6572
$\chi_2^h(1^3P_2)$	2^{-+}	11.3001	11.2704		0.6594
$h_b^h(2^1P_1)$	1^{--}	11.4775	11.4753	11.268(6)	0.9014
$\chi_0^h(2^3P_0)$	0^{-+}	11.4709	11.4728		0.8991
$\chi_1^h(2^3P_1)$	1^{-+}	11.4767	11.4753		0.9016
$\chi_2^h(2^3P_2)$	2^{-+}	11.48--	11.4763		0.9033
$h_b^h(3^1P_1)$	1^{--}	11.6393	11.6625		1.1139
$\chi_0^h(3^3P_0)$	0^{-+}	11.6322	11.6609		1.1127
$\chi_1^h(3^3P_1)$	1^{-+}	11.6384	11.6628		1.1145
$\chi_2^h(3^3P_2)$	2^{-+}	11.6422	11.6634		1.1154
$h_b^h(4^1P_1)$	1^{--}	11.7886	11.8361		1.3073
$\chi_0^h(4^3P_0)$	0^{-+}	11.7813	11.8350		1.3066
$\chi_1^h(4^3P_1)$	1^{-+}	11.7876	11.8366		1.3080
$\chi_2^h(4^3P_2)$	2^{-+}	11.7915	11.8370		1.3087
$h_b^h(5^1P_1)$	1^{--}	11.9283	11.9993		1.4871
$\chi_0^h(5^3P_0)$	0^{-+}	11.9210	11.9985		1.4867
$\chi_1^h(5^3P_1)$	1^{-+}	11.9273	11.9998		1.4879
$\chi_2^h(5^3P_2)$	2^{-+}	11.9313	12.0001		1.4885
$h_b^h(6^1P_1)$	1^{--}	12.0604	12.1540		1.6566
$\chi_0^h(6^3P_0)$	0^{-+}	12.0532	12.1535		1.6564
$\chi_1^h(6^3P_1)$	1^{-+}	12.0594	12.1547		1.6575
$\eta_{b2}(1^1D_2)$	2^{++}	11.3804	11.3619	11.117(4)	0.7561
$\Upsilon^h(1^3D_1)$	1^{+-}	11.3782	11.3583		0.7509
$\Upsilon_2^h(1^3D_2)$	2^{+-}	11.3803	11.3615		0.7553
$\Upsilon_3^h(1^3D_3)$	3^{+-}	11.3815	11.3637		0.7591
$\eta_{b2}^h(2^1D_2)$	2^{++}	11.5505	11.5584		0.9877
$\Upsilon^h(2^3D_1)$	1^{+-}	11.5474	11.5561		0.9846
$\Upsilon_2^h(2^3D_2)$	2^{+-}	11.5503	11.5583		0.9874
$\Upsilon_3^h(2^3D_3)$	3^{+-}	11.5522	11.5596		0.9896

4.2. Spectrum of Σ_u^- state

To check the validity of our model, masses of bottomonium mesons are calculated for Σ_u^- states. To calculate the mass of $b\bar{b}$ state, the constituent quark masses are added to the energy E , *i.e.*

$$m_{b\bar{b}} = 2m_b + E. \quad (13)$$

The lowest-order relativistic correction in mass is incorporated by perturbation theory as adopted in Refs. [7, 8]. With relativistic correction, the expression to calculate mass can be written as

$$m_{b\bar{b}} = 2m_b + E + \langle \Psi | \left(\frac{-1}{4m_b^3} \right) p^4 | \Psi \rangle. \quad (14)$$

The best fit values of parameters ($\alpha_s = 0.4$, $b = 0.11 \text{ GeV}^2$, $\sigma = 1 \text{ GeV}$, $m_b = 4.89 \text{ GeV}$) with relativistic correction are taken from Ref. [8]. The calculated masses for Σ_u^- states with and without relativistic corrections are reported in Table II.

4.3. Radii

The numerically calculated normalised wave functions are used to calculate the root mean square radii. To find the root mean square radii of the gluonic excited Σ_u^- bottomonium states, the following relation is used:

$$\sqrt{\langle r^2 \rangle} = \sqrt{\int U^* r^2 U dr}. \quad (15)$$

5. Discussion and conclusion

In this paper, a potential model for lowest-lying Σ_u^- hybrid states is proposed whose parameters are found by fitting the model with lattice data [5]. This model is used to calculate the numerical solutions of the Schrödinger equation for Σ_u^- states with different J^{PC} . In Figs. 2–3, normalised radial wave functions of Σ_g^+ and Σ_u^- states are plotted with respect to quark–antiquark separation r . Figures 2–3 show that peaks of radial wave functions are shifted away from the origin for gluonic excited states (Σ_u^-) comparing to gluonic ground states. Figure 2 shows that shape of wave functions is different for Σ_g^+ and Σ_u^- states for $L = 0$.

The newly suggested model is used to calculate the masses and radii of the Σ_u^- states and the results are written in Table II. Our calculated masses without relativistic corrections are close to the results given in Ref. [3] as shown in Table II. In Ref. [3], the spectrum is calculated without including the spin, so the same mass is given for η_b^h and Υ_b^h . However, our proposed

potential model gives distinguished results for $S = 0$ and $S = 1$. As observed from Table II, the lowest calculated mass of the Σ_u^- state is calculated to be 11.2012 GeV without relativistic corrections and is equal to 11.2378 GeV with the incorporation of relativistic corrections in masses. In Refs. [1, 5], the lowest mass of Σ_u^- state is 11.1 GeV. This shows that our calculated masses with non-relativistic corrections are closer to the masses calculated by lattice simulations [1, 5] than the relativistic masses.

From Table II, it is observed that masses and radii are increased by increasing the orbital quantum number (L). The similar behaviour is observed in Ref. [8] while working on Σ_g^+ and Π_u states of bottomonium meson. The spectrum of Σ_g^+ state bottomonium mesons is calculated in Ref. [8] by the shooting method and a few of the results of Ref. [8] are shown below in Table III. The comparison of masses of Σ_g^+ and Σ_u^- states shows that masses and radii of Σ_u^- states are greater than Σ_g^+ states. Overall, we conclude that masses and radii increase towards higher gluonic excitations.

TABLE III

Masses of Σ_g^+ states of bottomonium meson. These results are taken from our earlier work [8].

Meson	Relativistic mass	NR mass	$\sqrt{\langle r^2 \rangle}$
	GeV	GeV	fm
$\eta_b(1^1S_0)$	9.4926	9.5079	0.2265
$\Upsilon(1^3S_1)$	9.5098	9.5299	0.2328
$\eta_b(2^1S_0)$	10.0132	10.0041	0.5408
$\Upsilon(2^3S_1)$	10.0169	10.0101	0.5448
$h_b(1^1P_1)$	9.9672	9.9279	0.4347
$\chi_0(1^3P_0)$	9.8510	9.9232	0.4375
$\chi_1(1^3P_1)$	9.9612	9.9295	0.4379
$\chi_2(1^3P_2)$	9.9826	9.9326	0.4375
$\eta_{b2}(1^1D_2)$	10.1661	10.1355	0.5933
$\Upsilon(1^3D_1)$	10.1548	10.1299	0.5930
$\Upsilon_2(1^3D_2)$	10.1649	10.1351	0.5939
$\Upsilon_3(1^3D_3)$	10.1772	10.1389	0.5942

Our suggested potential model ($V_\Sigma(r)$) depends on parameters (A' , B' , P' , C'). The relative error in the masses due to $\pm 1\%$ change in each parameter (A' , B' , P' , C') is calculated to be within the range of (0.0096–0.0236)%, (0.0388–0.0861)%, (0.014–0.0223)%, (0.0789–0.0856)%, respectively. The standard deviation in masses is calculated to be equal to 0.303.

The results of calculated radial wave functions, masses and radii can be used to find more properties such as decay constant, decay widths and transition rates of gluonic excited Σ_u^- states. Overall, we conclude that our extended potential model can be used to study the gluonic excitations in a variety of meson sectors.

REFERENCES

- [1] K.J. Juge, J. Kuti, C. Morningstar, «Gluon excitations of the static quark potential and the hybrid quarkonium spectrum», *J. Nucl. Phys. Proc. Suppl.* **63**, 326 (1998).
- [2] G.S. Bali, A. Pineda, «QCD phenomenology of static sources and gluonic excitations at short distances», *Phys. Rev. D* **69**, 094001 (2004).
- [3] S. Capitani *et al.*, «Precision computation of hybrid static potentials in SU(3) lattice gauge theory», *Phys. Rev. D* **99**, 034502 (2019).
- [4] A.P. Szczepaniak, «Gluonic excitations and the GlueX experiment», *J. Phys.: Conf. Ser.* **9**, 315 (2005).
- [5] K.J. Juge, J. Kuti, C. Morningstar, «The heavy-quark hybrid meson spectrum in lattice QCD», *AIP Conf. Proc.* **688**, 193 (2003).
- [6] N. Akbar, B. Masud, S. Noor, «Wave-function-based characteristics of hybrid mesons», *Eur. Phys. J. A* **47**, 124 (2011); *Erratum ibid.* **50**, 121 (2014).
- [7] A. Sultan, N. Akbar, B. Masud, F. Akram, «Higher hybrid charmonia in an extended potential model», *Phys. Rev. D* **90**, 054001 (2014).
- [8] N. Akbar, M.A. Sultan, B. Masud, F. Akram, «Higher hybrid bottomonia in an extended potential model», *Phys. Rev. D* **95**, 074018 (2017).
- [9] N. Akbar, F. Akram, B. Masud, M.A. Sultan, «Conventional and hybrid B_c mesons in an extended potential model», *Eur. Phys. J. A* **55**, 82 (2019).
- [10] E. Braaten, C. Langmack, D.H. Smith, «Born–Oppenheimer approximation for the XYZ mesons», *Phys. Rev. D* **90**, 014044 (2014).
- [11] F. Iddir, L. Sendlala, «Hybrid States from Constituent Glue Model», *Int. J. Mod. Phys. A* **23**, 5229 (2008).
- [12] F. Iddir, L. Sendlala, «Heavy Hybrid Mesons Masses», arXiv:hep-ph/0611165.
- [13] F. Iddir, L. Sendlala, «Theoretical investigations on the Y(4260) being an hybrid meson», arXiv:hep-ph/0611183.
- [14] N. Brambilla, W.K. Lai, J. Segovia, J.T. Castellà, «QCD spin effects in the heavy hybrid potentials and spectra», *Phys. Rev. D* **101**, 054040 (2020).
- [15] R. Berg, D. Harnett, R.T. Kleiv, T.G. Steele, «Mass predictions for pseudoscalar ($J^{PC} = 0^{+-}$) charmonium and bottomonium hybrids in QCD sum-rules», *Phys. Rev. D* **86**, 034002 (2012).

- [16] D. Harnett, R. Berg, R.T. Kleiv, T.G. Steele, «A Laplace Sum-Rules Analysis of Heavy Pseudoscalar ($J^{PC} = 0^{+-}$) Hybrids», *Nucl. Phys. B Proc. Suppl.* **234**, 154 (2013).
- [17] D. Harnett, R.T. Kleiv, T.G. Steele, H.y. Jin, «Axial vector ($J^{PC} = 1^{++}$) charmonium and bottomonium hybrid mass predictions with QCD sum-rules», *J. Phys. G: Nucl. Part. Phys.* **39**, 125003 (2012).
- [18] R.T. Kleiv, D. Harnett, T.G. Steele, H.y. Jin, « $J^{PC} = 1^{++}$ heavy hybrid masses from QCD sum-rules», *Nucl. Phys. B. Proc. Suppl.* **234**, 150 (2013).
- [19] R.T. Kleiv *et al.*, «A survey of the number of legally blind university physics students in Canada during 2003–2013», *Can. J. Phys.* **93**, 1 (2015).
- [20] W. Chen *et al.*, «Exotic Hadron States», Proceedings, 30th International Workshop on High Energy Physics: Particle and Astroparticle Physics, Gravitation and Cosmology: Predictions, Observations and New Projects (IHEP 2014): Protvino, Russia, June 23–27, 2014.
- [21] C.F. Qiaoa, L. Tang, G. Hao, Xue-Qian Li, «Determining 1^{--} heavy hybrid masses via QCD sum rules», *J. Phys. G: Nucl. Part. Phys.* **39**, 015005 (2012).
- [22] W. Chen, T.G. Steele, Shi-Lin Zhu, «Heavy tetraquark states and quarkonium hybrids», *Universe* **2**, 13 (2014), arXiv:1403.7457 [hep-ph].
- [23] J.Y. Cui, H.Y. Jin, J.M. Wu, «The Spectrum of the Hybrid Mesons with Heavy Quarks from the BS Equation», *Int. J. Mod. Phys. A* **14**, 2273 (1999).
- [24] T. Barnes, S. Godfrey, E.S. Swanson, «Higher charmonia», *Phys. Rev. D* **72**, 054026 (2005).
- [25] S. Godfrey, N. Isgur, «Mesons in a relativized quark model with chromodynamics», *Phys. Rev. D* **32**, 189 (1985).